Visualizing a bosonic symmetry protected topological phase in an interacting fermion model

Han-Qing Wu, Yuan-Yao He, Yi-Zhuang You, Tsuneya Yoshida, Norio Kawakami, Cenke Xu, Zi Yang Meng, and Zhong-Yi Lu

Phys. Rev. B **94**, 165121 — Published 11 October 2016

DOI: 10.1103/PhysRevB.94.165121

Visualizing a Bosonic Symmetry Protected Topological Phase in an Interacting Fermion Model

Han-Qing Wu,[1] Yuan-Yao He,[1] Yi-Zhuang You,[2] Tsuneya Yoshida,[3] Norio Kawakami,[3] Cenke Xu,[2] Zi Yang Meng,[4] and Zhong-Yi Lu[1]

[1] *Department of Physics, Renmin University of China, Beijing 100872, China*
[2] *Department of Physics, University of California, Santa Barbara, California 93106, USA*
[3] *Department of Physics, Kyoto University, Kyoto 606-8502, Japan*
[4] *Beijing National Laboratory for Condensed Matter Physics, and Institute of Physics, Chinese Academy of Sciences, Beijing 100190, China*

(Dated: July 6, 2016)

Symmetry protected topological (SPT) phases in free fermion and interacting bosonic systems have been classified, but the physical phenomena of interacting fermionic SPT phases have not been fully explored. Here, employing large-scale quantum Monte Carlo simulation, we investigate the edge physics of a bilayer Kane-Mele-Hubbard model with zigzag ribbon geometry. Our unbiased numerical results show that the fermion edge modes are gapped out by interaction, while the bosonic edge modes remain gapless at the $(1+1)d$ boundary, before the bulk quantum phase transition to a topologically trivial phase. Therefore, finite fermion gaps both in the bulk and on the edge, together with the robust gapless bosonic edge modes, prove that our system becomes an emergent bosonic SPT phase at low energy, which is, for the first time, directly observed in an interacting fermion lattice model.

PACS numbers: 71.10.Fd, 71.27.+a, 73.43.-f

Introduction. Symmetry protected topological (SPT) phases are bulk gapped states with either gapless or degenerate edge excitations protected by symmetries. The SPT phases in free fermion systems, like topological insulators [1–5], acquire metallic edge states and have been fully classified [6, 7]. On the other hand, although bosonic SPT phases have been formally classified and constructed as well from group cohomology [8, 9] and field theories [10–13], there has been little study about realization of bosonic SPT states in condensed matter systems, except for the well-known $1d$ Haldane phase that is realized in a spin-1 Heisenberg model [14, 15] and some proposals of realizing a $2d$ bosonic SPT state in cold atom systems [16]. Using the same "flux-attachment" picture as Ref. 16, lattice models of bosonic integer quantum Hall states have been studied [17–21].

Recently it was proposed that instead of directly studying bosonic systems, the physics of bosonic SPT states can be mimicked by interacting fermionic systems, in the sense that its low energy physics is completely identical to bosonic SPT states [22]. For example, in an interacting fermion model on the AA-stacked bilayer Kane-Mele-Hubbard model, a *bona fide* interaction-driven topological phase transition has been studied in our previous papers [23–25]. A direct continuous quantum phase transition between a quantum spin Hall (QSH) phase and a topologically trivial Mott insulator was found via large-scale quantum Monte Carlo (QMC) simulations. At the critical point, only the bosonic spin and charge gaps are closed, while the bulk single-particle excitations remain open. This transition can be described by a $(2+1)d$ $O(4)$ nonlinear sigma model with a topological Θ-term [23, 24, 26]. However, as for the physics on

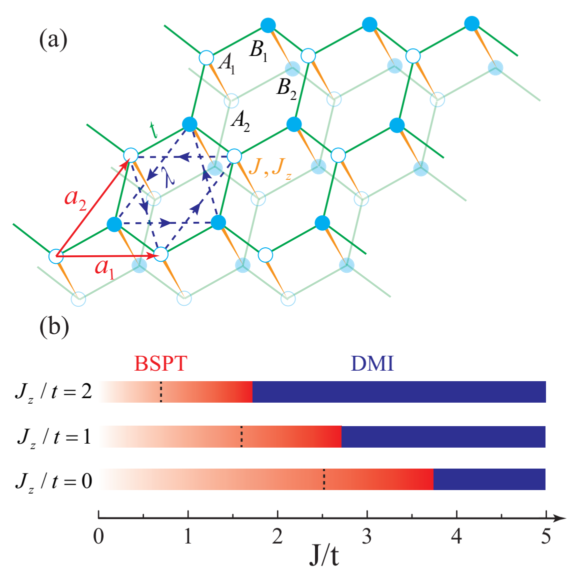

FIG. 1. (Color online) (a) Illustration of AA-stacked honeycomb ribbon ($L_{\mathbf{a}_1} = 3$, $L_{\mathbf{a}_2} = 3$) with periodic (open) boundary condition along $\mathbf{a}_1$ ($\mathbf{a}_2$) direction. $\mathbf{a}_1 = (1, 0)$ and $\mathbf{a}_2 = (1/2, \sqrt{3}/2)$ are the primitive translation vectors. A_1, B_1, A_2 and B_2 are the four sublattices within one unit cell. (b) J-J_z phase diagram of bilayer Kane-Mele-Hubbard model. The bosonic SPT (BSPT, red) and dimer Mott insulator (DMI, blue) phases are separated by a bulk transition. The dashed lines inside BSPT denote the J values, above which one can clearly see the exponential decay of the single-particle Green's function at the boundary from our finite-size calculations. The relative range of such region becomes wider as J_z increases.

the edge, although the field theory and renormalization group analysis [27] provide us with analytical evidence of gapless bosonic edge, which is supported by an extended version of dynamical mean-field theory calculation at finite temperatures[28], unbiased numerical evidence that can prove the conclusion is still demanded, and it is the task of this paper.

Here, we employ large-scale QMC simulation to the zigzag ribbon geometry, i.e., the bilayer Kane-Mele-Hubbard model with periodic boundary condition along $\mathbf{a}_1$ direction and open boundary along $\mathbf{a}_2$ direction (see Fig. 1 (a)). On finite-size ribbon, our unbiased results unveil a substantial region ($\sim t$) of bosonic SPT phase from the exponential decay of the single-particle Green's function along the boundary before the bulk quantum phase transition, while the gapless $O(4)$ bosonic modes prevail on the edge with power-law correlation functions.

Model and Method. The Hamiltonian [24, 27] of the AA-stacked bilayer Kane-Mele-Hubbard model is given by

$$\begin{aligned}\hat{H} = &-t \sum_{\xi\langle i,j\rangle\alpha} (\hat{c}^{\dagger}_{\xi i\alpha}\hat{c}_{\xi j\alpha} + \hat{c}^{\dagger}_{\xi j\alpha}\hat{c}_{\xi i\alpha}) \\ &+ i\lambda \sum_{\xi\langle\langle i,j\rangle\rangle\alpha\beta} \nu_{ij}(\hat{c}^{\dagger}_{\xi i\alpha}\sigma^{z}_{\alpha\beta}\hat{c}_{\xi j\beta} - \hat{c}^{\dagger}_{\xi j\beta}\sigma^{z}_{\beta\alpha}\hat{c}_{\xi i\alpha}) \\ &- \frac{J}{8}\sum_{i}\left[(\hat{D}_{1i,2i} + \hat{D}^{\dagger}_{1i,2i})^2 - (\hat{D}_{1i,2i} - \hat{D}^{\dagger}_{1i,2i})^2\right] \\ &- \frac{J_z}{4}\sum_{i}\left[(\hat{n}_{1i\uparrow} - \hat{n}_{1i\downarrow}) - (\hat{n}_{2i\uparrow} - \hat{n}_{2i\downarrow})\right]^2,\end{aligned} \tag{1}$$

with $\hat{D}_{1i,2i} = \sum_{\sigma}\hat{c}^{\dagger}_{1i\sigma}\hat{c}_{2i\sigma}$. Here α, β denote the spin species and $\xi = 1, 2$ stand for the layer index. The first term in Eq. (1) describes the nearest-neighbor hopping (green lines in Fig. 1 (a)) and the second term represents spin-orbital coupling $\lambda/t = 0.2$ (blue lines with arrows in Fig. 1 (a)). The third term J is the interlayer antiferromagnetic Heisenberg (approximated) interaction [24], and the last term J_z denotes the interlayer antiferromagnetic Ising (approximated) interaction [27]. When $J/t > 0$ and $J_z/t > 0$, we can prove that there is no fermion sign problem in the QMC calculations [27].

This Hamiltonian possesses a high symmetry, $SO(4) \times SO(3)$ [24, 27]. When $J_z/t = 0$, in the bulk, J drives a continuous quantum phase transition from a quantum spin Hall (QSH) phase to an interlayer dimer phase at $J_c/t \approx 3.73$, and since there is no spontaneous symmetry breaking at both sides of this transition, it is dubbed as a *bona fide* interaction-driven topological phase transition [24]. On the other hand, when $J/t = 0$, it is perceivable that J_z will eventually drive the system into a spin-density-wave phase with magnetization along z direction (SDW-Z) which spontaneously breaks the $SO(3)$ symmetry and time-reversal symmetry. Our numerical data shows that the SDW-Z order establishes when $J_z/t > 2$. More information about the $J-J_z$ phase diagram is given in Supplemental Material [29].

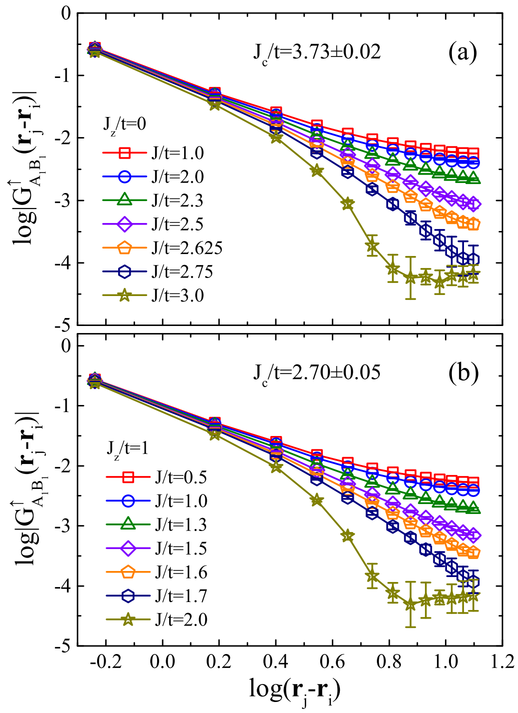

FIG. 2. (Color online) The log-log plot of single-particle Green's function at the boundary as a function of interlayer antiferromagnetic interaction J/t when (a) $J_z/t = 0$ and (b) $J_z/t = 1$. In both cases, results show the exponential decay before the bulk topological phase transition J_c/t.

The QSH phase still survives when the interlayer interactions are not sufficiently strong. However, we will show that the gapless edge modes in the interacting QSH phase are carried by bosons emerging from interacting fermionic degrees of freedoms, hence the system is actually in a bosonic SPT state before the bulk phase transition (the BSPT phase in Fig. 1 (b)). This conclusion is drawn upon the numerical observation of exponential decay of single-particle Green's function on the edge before the bulk quantum phase transition, while at the same time bosonic $O(4)$ correlation functions present a clear power-law decay.

The QMC method employed here is the projective auxiliary-field quantum Monte Carlo approach [30, 31]. It is a zero-temperature version of the determinantal QMC algorithm. The specific implementation of the QMC method on the model in Eq. (1) is presented in Ref. [24]. The projection parameter is chosen at $\Theta = 50/t$ and the Trotter slice $\Delta\tau = 0.05/t$. Since the gapless edge modes are hallmarks of SPTs, we perform the simulation with periodic (open) boundary condition along $\mathbf{a}_1$ ($\mathbf{a}_2$) direction (see Fig. 1 (a)). The main results in this paper are obtained from a ribbon with $L_{\mathbf{a}_1} = 27, L_{\mathbf{a}_2} = 9$ which is large enough to obtain controlled representation of thermodynamic limit behaviors of BSPT phase in Fig. 1 (b).

Edge analysis. In the non-interacting limit, the bilayer Kane-Mele model supports four fermionic edge modes: two left-moving up-spin modes and two right-moving down-spin modes from both layers, respectively. They are denoted by the boundary fermion fields $c_{\xi\alpha}$ ($\xi = 1, 2$, $\alpha = \uparrow, \downarrow$). Following the standard Abelian bosonization procedure, we can rewrite $c_{\xi\alpha} = \kappa_{\xi\alpha} e^{i\phi_{\xi\alpha}}/\sqrt{2\pi a}$, where a is a short distance cut-off and $\kappa_{\xi\alpha}$ is the Klein factor that ensures the anticommutation of the fermion operators. As we turn on the interaction, in terms of the bosonized degrees of freedom $\phi = (\phi_{1\uparrow}, \phi_{2\uparrow}, \phi_{1\downarrow}, \phi_{2\downarrow})$, the effective action for the interacting edge modes reads

$$S = \int d\tau dx \frac{1}{4\pi}(\partial_x \phi^\intercal K \partial_\tau \phi + \partial_x \phi^\intercal V \partial_x \phi) - \lambda \cos(l_0^\intercal \phi),$$

$$K = \begin{pmatrix} 1 & & & \\ & 1 & & \\ & & -1 & \\ & & & -1 \end{pmatrix}, V = v_0 \begin{pmatrix} 1 & u & -g & g \\ u & 1 & g & -g \\ -g & g & 1 & u \\ g & -g & u & 1 \end{pmatrix}, \tag{2}$$

where $g = J_z/(4\pi v_0 - J_z)$, $u = (J_z + J)/(4\pi v_0 - J_z)$ and v_0 is the bare velocity of the edge modes. $\lambda \propto J$ is the backscattering term induced by the interlayer Heisenberg interaction with the corresponding charge vector $l_0 = (1, -1, -1, 1)^\intercal$. The scaling dimension of $\cos(l_0^\intercal \phi)$ is

$$\Delta_0 = \frac{2(1 - u - 2g)}{\sqrt{(1-u)^2 - 4g^2}}. \tag{3}$$

Without the Ising interaction J_z (i.e. $g \to 0$), the operator $\cos(l_0^\intercal \phi)$ is marginal from the scaling dimension $\Delta_0 = 2$. Further renormalization group (RG) analysis[27] shows that the term $\lambda \cos(l_0^\intercal \phi)$ is marginally relevant, meaning that the fermionic edge modes of the non-interacting QSH state are unstable to the interaction J. As long as J is turned on, the boundary fermions will be gapped out by the interaction, leaving only bosonic edge modes described by the spin $c_{1\uparrow}^\dagger c_{1\downarrow} - c_{2\uparrow}^\dagger c_{2\downarrow}$ and charge $c_{1\uparrow} c_{2\downarrow} - c_{1\downarrow} c_{2\uparrow}$ fluctuations. However, due to the marginal nature of RG flow, the boundary fermion gap could be very small for small J, which is hard to resolve in our finite-size numerical study. The positive J_z interaction (i.e. $g > 0$) helps to boost the RG flow by reducing the scaling dimension Δ_0 according to Eq. (3), such that J becomes relevant and the gap in the single-particle (fermionic) spectrum can be observed in numerics for smaller J as well. In the following, we will show that with moderate interaction J, the QSH edge modes indeed become bosonic at low energy, resembling the key feature of BSPT states. The interaction J_z will help to enhance the fermion gap and make the BSPT edge modes more prominent in a finite-size system.

Numerical results. Figures 2 (a) and (b) show the single-particle Green's function $G_{ij}^\sigma = \langle\Psi| \hat{c}_{i\sigma}^\dagger \hat{c}_{j\sigma} |\Psi\rangle / \langle\Psi|\Psi\rangle$ along the edge as a function of J/t, at $J_z/t = 0$ and 1, respectively. $|\Psi\rangle \propto e^{-\Theta \hat{H}/2} |\Psi_T\rangle$ is the ground state wave function projected from a trial

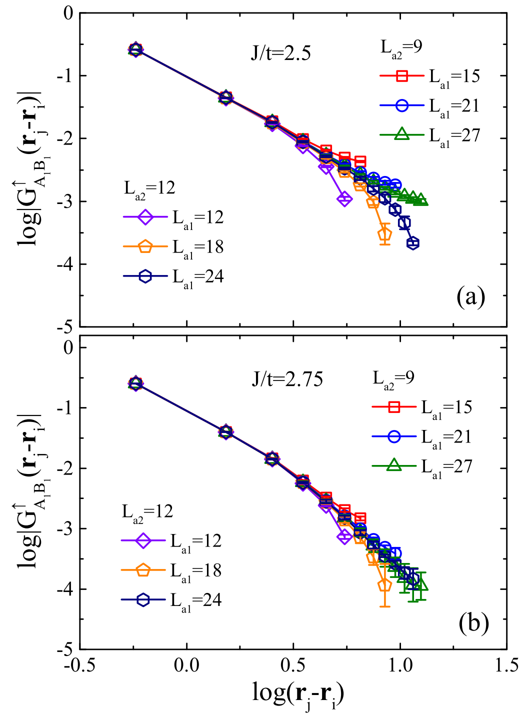

FIG. 3. Illustration of finite-size effects in the single-particle Green's function along edge for different $L_{\mathbf{a}_1}$ and $L_{\mathbf{a}_2}$. (a) at $J/t = 2.5, J_z/t = 0$, the exponential decay of the single-particle Green's function accquires strong finite-size effect. (b) at $J/t = 2.75, J_z/t = 0$, the finite size effect is absent and exponential decay is seen for the chosen $L_{\mathbf{a}_1}$ and $L_{\mathbf{a}_2}$.

wave function $|\Psi_T\rangle$ [24]. We see a clear exponential decay before the bulk transition at $J_c/t \approx 3.73$ (for $J_z/t = 0$) and $J_c/t \approx 2.7$ (for $J_z/t = 1$). The exponential decay of edge single-particle Green's function at $J < J_c$ indicates that fermions are no longer gapless at the boundary between our model system and a topologically trivial one (such as vacuum).

To rule out the possible finite-size effect, we employ several different ribbon geometries in the QMC calculations. From Fig. 3 (a), it is hard to determine whether the edge single-particle Green's function will exponentially decay in the thermodynamic limit when $J/t = 2.5, J_z/t = 0$ because of the strong finite-size effect. However, when $J/t = 2.75, J_z/t = 0$, we see a clear exponential decay no matter if $L_{\mathbf{a}_1}$ and $L_{\mathbf{a}_2}$ are even or odd, large or small, and the single-particle Green's function has a clear trend to truly exponential decay in the thermodynamic limit.

The exponential decay of single-particle Green's function at the boundary in the thermodynamic limit indicates that the gapless fermion edge mode in the non-interacting case is gapped out by the interlayer exchange interaction. Hence the fermion excitations have a gap both in the bulk and on the edge [24]. However, as shown in our edge analysis, the system can still be non-trivial in

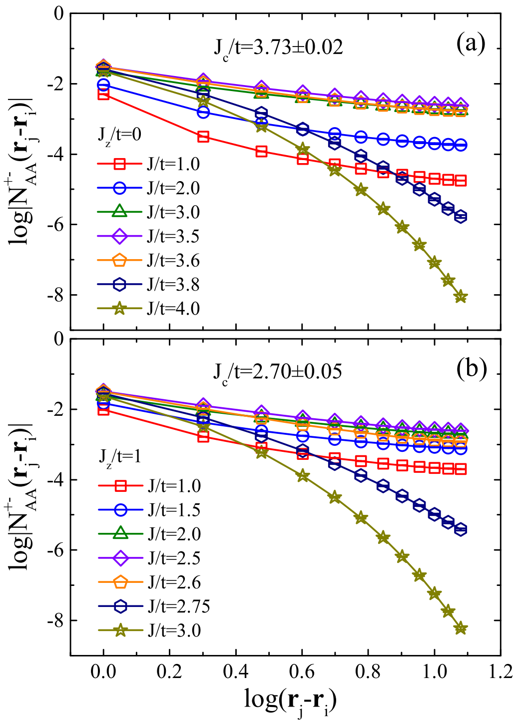

FIG. 4. (Color online) The log-log plot of equal-time two-particle $O(4)$ vector correlation function at the boundary for (a) $J_z/t = 0$ and (b) $J_z/t = 1$. Both panels show the power-law decay behaviors before the bulk topological phase transition at J_c/t.

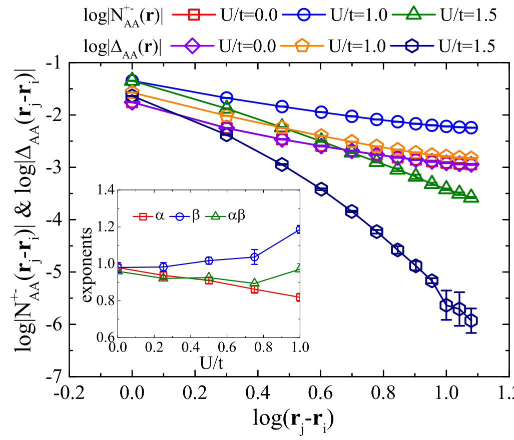

FIG. 5. (Color online) Edge spin $N^{+-}_{AA}(\mathbf{r})$ and pairing $\Delta_{A_1A_2}(\mathbf{r})$ correlation functions for increasing U/t, at $J/t = 2.75$ and $J_z/t = 0$. Inset shows the extracted Luttinger parameters as a function of U/t.

the bosonic sector [27]. To see this, we calculate the XY spin (SDW-XY) correlation function and superconducting pairing (SC) correlation function at the boundary. According to the analysis in Ref. [27], we define them as

$$N^{+-}_{AA}(\mathbf{r}_j-\mathbf{r}_i) = \frac{1}{2}[S^{\pm}_{A_1A_1}(\mathbf{r}_j-\mathbf{r}_i) - S^{\pm}_{A_1A_2}(\mathbf{r}_j-\mathbf{r}_i) - S^{\pm}_{A_2A_1}(\mathbf{r}_j-\mathbf{r}_i) + S^{\pm}_{A_2A_2}(\mathbf{r}_j-\mathbf{r}_i)]$$

$$\Delta_{AA}(\mathbf{r}_j-\mathbf{r}_i) = \langle\Psi|\,\hat{\Delta}^{\dagger}_{iA_1A_2}\hat{\Delta}_{jA_1A_2}\,|\Psi\rangle\,/\,\langle\Psi|\Psi\rangle \qquad (4)$$

where $S^{\pm}_{mn}(\mathbf{r}_j-\mathbf{r}_i) = \langle\Psi|\,\frac{1}{2}(\hat{S}^+_i\hat{S}^-_j + \hat{S}^-_i\hat{S}^+_j)\,|\Psi\rangle\,/\,\langle\Psi|\Psi\rangle$, $m, n = A_1, A_2$ denote the A sublattice sites in the first and second layer. i and j label the unit cells. $\hat{S}^+_i$ is the spin flip operator and $\hat{\Delta}^{\dagger}_{iA_1A_2}$ is the interlayer singlet creation operator. Fig. 4 (a) and (b) show the SDW-XY correlation function at the boundary as a function of J/t. Before the bulk quantum phase transition, they all show the power-law decay at $J < J_c$. Due to the $SO(4)$ symmetry, the SDW-XY and SC correlation function is exactly the same because they rotate into each other [24, 27]. So the physical bosonic boundary modes are simply the SDW-XY and SC fluctuations on the boundary.

Turning on an extra on-site Hubbard interaction $U\sum_i(\hat{n}_{i\uparrow}+\hat{n}_{i\downarrow}-1)^2$ (see Sec. VII in Supplemental Material [29] for the U/t path chosen in the bulk phase diagram) to our original model Eq. (1) would break the $O(4)$ symmetry, and change the scaling dimension of the spin and Cooper pair operators. According to the bosonization analysis in Ref. [27], the spin and pairing $O(4)$ bosonic modes always have power-law correlation, with $N^{+-}_{AA}(\mathbf{r}) \propto |\mathbf{r}|^{-\alpha}$ and $\Delta_{AA}(\mathbf{r}) \propto |\mathbf{r}|^{-\beta}$. α and β depend on the Luttinger parameters, but their product remains a universal constant: $\alpha\beta = 1$. This is due to the fact that, spin and charge are a pair of conjugate variables at the boundary, which is a physical consequence of the SPT state in the bulk. This prediction is confirmed in our simulation. In Fig. 5, at $J/t = 2.75$ $J_z/t = 0$ and gradually increasing U/t, $N^{+-}_{AA}(\mathbf{r})$ and $\Delta_{AA}(\mathbf{r})$ have the same power law $\alpha = \beta \sim 1$ at $U/t = 0$, but as U/t increases, α and β start to deviate, but their product $\alpha\beta$ remains close to 1, as shown in the inset of Fig. 5, till the bulk transition to a SDW-XY phase at $U_c/t \sim 1.3$ [24, 29].

Discussion. In this Letter, we have performed QMC simulation for a proposed interacting lattice fermion model, and explicitly demonstrated that this system shows a bosonic SPT state, in the sense that the boundary has gapless bosonic modes, but no gapless fermionic modes under interaction. Recently it was also proposed that the same physics can be realized in an AB stacking bilayer graphene under a strong out-of-plane magnetic field and Coulomb interaction [32]. Our model, though technically different, should belong to the same topological class, and it has the advantage of being sign problem free for QMC simulation. Unbiased information of such strongly correlated system, including transport and spectral properties, can be obtained from QMC simulation, and quantitative comparison with the up-coming experiments are hence made possible.

The numerical calculations were carried out at the National Supercomputer Center in Guangzhou on the Tianhe-2 platform. H.Q.W., Y.Y.H. and Z.Y.L. acknowledge support from the National Natural Science

Foundation of China (NSFC Grant Nos. 11474356 and 91421304) and Special Program for Applied Research on SuperComputation of the NSFC-Guangdong Joint Fund (the second phase). C.X. and Y.Z.Y. are supported by the David and Lucile Packard Foundation and NSF Grant No. DMR-1151208. Z.Y.M. is supported by the National Thousand-Young-Talents Program of China as well as NSFC Grant Nos. 11421092 and 11574359. T.Y. and N.K. are supported by JSPS KAKENHI No. 15H05855.

[1] C. L. Kane and E. J. Mele, Phys. Rev. Lett. **95**, 146802 (2005).
[2] C. L. Kane and E. J. Mele, Phys. Rev. Lett. **95**, 226801 (2005).
[3] L. Fu, C. L. Kane, and E. J. Mele, Phys. Rev. Lett. **98**, 106803 (2007).
[4] J. E. Moore and L. Balents, Phys. Rev. B **75**, 121306 (2007).
[5] R. Roy, Phys. Rev. B **79**, 195322 (2009).
[6] A. P. Schnyder, S. Ryu, A. Furusaki, and A. W. W. Ludwig, AIP Conference Proceedings **1134**, 10 (2009).
[7] A. Kitaev, AIP Conference Proceedings **1134**, 22 (2009).
[8] X. Chen, Z.-C. Gu, Z.-X. Liu, and X.-G. Wen, Science **338**, 1604 (2012), http://science.sciencemag.org/content/338/6114/1604.full.pdf.
[9] X. Chen, Z.-C. Gu, Z.-X. Liu, and X.-G. Wen, Phys. Rev. B **87**, 155114 (2013).
[10] Y.-M. Lu and A. Vishwanath, Phys. Rev. B **86**, 125119 (2012).
[11] A. Vishwanath and T. Senthil, Phys. Rev. X **3**, 011016 (2013).
[12] C. Xu and T. Senthil, Phys. Rev. B **87**, 174412 (2013).
[13] Z. Bi, A. Rasmussen, K. Slagle, and C. Xu, Phys. Rev. B **91**, 134404 (2015).
[14] F. D. M. Haldane, Phys. Lett. A **93**, 464 (1983).
[15] F. D. M. Haldane, Phys. Rev. Lett. **50**, 1153 (1983).
[16] T. Senthil and M. Levin, Phys. Rev. Lett. **110**, 046801 (2013).
[17] S. Furukawa and M. Ueda, Phys. Rev. Lett. **111**, 090401 (2013).
[18] Y.-C. He, S. Bhattacharjee, R. Moessner, and F. Pollmann, Phys. Rev. Lett. **115**, 116803 (2015).
[19] A. Sterdyniak, N. R. Cooper, and N. Regnault, Phys. Rev. Lett. **115**, 116802 (2015).
[20] Y. Fuji, Y.-C. He, S. Bhattacharjee, and F. Pollmann, Phys. Rev. B **93**, 195143 (2016).
[21] T.-S. Zeng, W. Zhu, and D. N. Sheng, Phys. Rev. B **93**, 195121 (2016).
[22] Y.-Z. You, Z. Bi, A. Rasmussen, M. Cheng, and C. Xu, New Journal of Physics **17**, 075010 (2015).
[23] K. Slagle, Y.-Z. You, and C. Xu, Phys. Rev. B **91**, 115121 (2015).
[24] Y.-Y. He, H.-Q. Wu, Y.-Z. You, C. Xu, Z. Y. Meng, and Z.-Y. Lu, Phys. Rev. B **93**, 115150 (2016).
[25] Y.-Y. He, H.-Q. Wu, Z. Y. Meng, and Z.-Y. Lu, Phys. Rev. B **93**, 195164 (2016).
[26] C. Xu and A. W. W. Ludwig, Phys. Rev. Lett. **110**, 200405 (2013).
[27] Y.-Z. You, Z. Bi, D. Mao, and C. Xu, Phys. Rev. B **93**, 125101 (2016).
[28] T. Yoshida and N. Kawakami, arXiv **1604**, 00122 (2016).
[29] See Supplemental Material for details on $J_z > 0$ results, the SDW-Z phase, finite size effect of the ribbon geometry, the effect of U interaction, etc.
[30] F. Assaad and H. Evertz, in Computational Many-Particle Physics, Lecture Notes in Physics, Vol. 739, edited by H. Fehske, R. Schneider, and A. Weiße (Springer Berlin Heidelberg, 2008) pp. 277–356.
[31] Z. Y. Meng, T. C. Lang, S. Wessel, F. F. Assaad, and A. Muramatsu, Nature **464**, 847 (2010).
[32] B. Zhen, Z. Ruixing, Y. Yi-Zhuang, Y. Andrea, B. Leon, L. Chao-Xing, and X. Cenke, arXiv **1602**, 03190 (2016).